Research Article **Open Access**

Noémi Kántor*, Attila Kovács, and Ágnes Takács

Small-scale human-biometeorological impacts of shading by a large tree

DOI 10.1515/geo-2016-0021

Received August 27, 2015; accepted December 21, 2015

Abstract: This study provides evidences on the beneficial small-scale human-biometeorological effects of a large shade tree during the daytime in summer. We carried out detailed measurement from 10 am to 6 pm with two human-biometeorological stations on a popular square in Szeged, Hungary. One of the stations stood under a great *Sophora japonica*, while the other in the sun. Compared to the sunny location, we found 0.5°C lower air temperature, 2% higher relative humidity and 0.4 hPa higher vapor pressure under the tree. From human-biometeorological point of view, we observed more significant differences. The tree reduced the mean radiant temperature by 22.1°C and the physiological equivalent temperature by 9.3°C - indicating about two categories lower physiological stress on the human body. In order to demonstrate the background mechanisms of these differences, we analyzed separately the components of the radiation budget. The effect of tree crown on radiation components was found to be greater in the short-wave domain than in the long-wave domain. The extended foliage reduced the solar radiation from the upper hemisphere and thus lowered the radiation from the ground (the reflected short-wave and the emitted long-wave flux densities) along with the radiation from the lateral directions.

Keywords: urban tree; shading; heat stress reduction; physiologically equivalent temperature

1 Introduction

According to regional climate model projections, Central-Europe will experience higher air temperature values and more intense heat waves in the future. In addition, extreme heat events are predicted to become more frequent and longer lasting [1, 2]. As a consequence, heat wave induced heat stress will likely lead to increased mortality, especially among heat-sensitive groups like infants and elderly people [3, 4]. The negative effects of extreme heat waves on human health, overall well-being and work performance are generally more intense in urban areas where large-scale meteorological conditions are exacerbated by local hot spots owing to the predominance of artificial materials, complex surface geometries, and to air pollution. Recent studies also reported that summertime heat stress may increase much more in cities than in rural and natural areas [5, 6].

In the light of the predicted warming trends[1] and the excessive level urbanization[2], there is an emerging need for thermal stress reduction in the urban environment. Therefore, the need for climate conscious urban planning and landscape design strategies is greater than ever before. It is necessary that planners and designers take into consideration the special features of urban microclimates and their human-biometeorological effects [7–10]. However, adequate planning strategies for heat stress mitigation and human thermal comfort enhancement necessitate both qualitative and quantitative information on the parameters and mechanisms that influence human heat balance and thereby human well-being and health.

Studies on the role of green infrastructure in cities are especially important to develop appropriate adaptation strategies [11, 12]. Beside other beneficial ecosystem services, trees exert a significant climate-modification effect - be it a single tree or a cluster of trees. Early studies on the climate regulation services of urban vegetation primarily focused on their air temperature reduction capacities [13]. However, some researchers have recognized the significance of human-biometeorological assessment that considers the effect of several meteorological parameters on the human body when evaluating urban environ-

***Corresponding Author: Noémi Kántor:** University of Szeged, Szeged, Hungary

Attila Kovács, Ágnes Takács: University of Szeged, Szeged, Hungary

1 IPCC, Climate Change 2014: Synthesis Report, 2014, http://www.ipcc.ch/pdf/assessment-report/ar5/syr/SYR_AR5_FINAL_full.pdf

2 UNFPA, The state of world population 2011. Report of the United Nations Population Fund. United Nations Population Fund, New York, 2011.

ments [14–23]. As a result, the number of studies that go beyond the mere air temperature lowering effect of trees by putting more emphasis on parameters that influence the heat balance of humans is continuously growing [24–29]. According to these studies, radiation is the key parameter that drives human-biometeorological indices - especially in warm and sunny conditions. Thus, it is of great importance to gather scientific evidences on the radiation-modification effect of different landscape planning strategies, especially on the heat stress mitigation potential of urban trees.

The objective of our study is to provide evidences on the beneficial micro-meteorological modification effect of large urban trees with an emphasis on their human-biometeorological effects. Since the number of detailed field studies is still rather low, we hope to encourage more scientists to perform similar investigations by paying special attention to the human-biometeorological concept and to the measurement design. We seek to illustrate our findings in a comprehensive manner that is easy to understand both by researchers and by members of other disciplines, such as landscape architects, urban planners and policy makers.

2 Methods

2.1 Study area and measurement design

Szeged is the largest city in the southeastern region of Hungary (46°N, 20°E, 82 m above sea level) with a population of about 162,000. Szeged is characterized by a dry-warm continental climate with drought susceptible summers. Based on the 1961-1990 climate normal period, the yearly sunshine duration is around 2000 hours, the annual mean air temperature is 10.5°C and the annual sum of precipitation is below 500 mm [30] (Appendix 1). Mean air temperature values are around 20°C during the summer months (June, July and August) with maximum air temperature values exceeding 25°C. In this season, the vapor pressure is 15-16 hPa and the relative humidity is slightly below 70% [30].

The study area is a medium-sized (7500 m^2) recreational place in the city center, called Dugonics Square (Appendix 2). The main reason for selecting this square as study area is that a large number of visitors attend it daily. Thanks to its complete reconstruction the square received the Award of Excellence from the Hungarian Society for Urban Planning in 2014. Moreover, the square lies on flat land that enables our results to be generalized, as they are devoid of topographical influences [24]. The square is surrounded with 2 to 4 storey (8-13 m height) buildings, similarly to other open places in the downtown of Szeged. The ground cover is evenly divided between artificial materials (dark red paving stones and resin bound pea gravel) and large grassy areas with flower beds.

We selected a large, mature tree on the square in order to demonstrate the micro-meteorological effect of urban trees and their human-biometeorological significance. Utilizing two human-biometeorological stations we measured all atmospheric parameters that influence the human heat budget (Figure 1). One of the stations stood under the canopy of the tree and the other in an open location where it was exposed to solar radiation during our measurement periods. On-site measurements lasted from 10 am to 6 pm (Central European Summer Time) on five selected days in May and June, 2015. We chose this time of the year, since the daytime air temperature generally exceeds 25°C and the solar radiation is the strongest.

The selected tree was a pagoda tree (*Sophora japonica*) - a species with large but sparse canopy - that is frequently used as street and park tree in Central Europe. The tree has a height of 11.5 m, a trunk height of 2.5 m, a canopy diameter of 13 m and its trunk inclines by 40° (Figure 1). The criterion for selecting a tree, as subject of our study, was that its crown remained unshaded by other landscape elements and thus received direct solar radiation during the measurement campaign. Our site selection criteria also included that the two measurement locations have good ventilation without considerable wind obstacles around them and that they are located relatively close to each other. In this way, observed human-biometeorological differences remained uninfluenced by wind sheltering or at most they were influenced equally.

At both location, Vaisala WXT 520 weather transmitters recorded air temperature (T_a [°C]), relative humidity (RH [%]) and wind velocity (v [m/s]). The accuracy of these measured parameters are presented in Table 1. We utilized Kipp & Zonen net radiometers (CNR-1 and CNR-4) for short-wave and long-wave radiation measurements (K_i and L_i [W/m^2] respectively, where subscripts indicate one of the six spatial directions: up, down, north, south, east or west). Using the telescopic legs of the tripods, we placed the sensors at 1.1 m height above ground level. This height corresponds to the center of gravity of a standing European man, which is the most frequently applied standard subject in outdoor thermal comfort investigations [9, 18]. The instrument recorded 1-minute averages of all parameters. Later we calculated vapor pressure (VP [hPa]) from measured RH and T_a values.

Figure 1: Measurement design: one human-biometeorological station is in the sun, the other is under the crown of a large *Sophora japonica*; and fish-eye photos taken at the measuring points.

Table 1: Instrumentation of the two human-biometeorological stations.

measured parameters		sensors	accuracy
T_a [°C]	air temperature	Thermocap, WXT 520, Vaisala	±0.3°C at 20°C, ±0.25°C at 0°C
RH [%]	relative humidity	Humicap, WXT 520, Vaisala	±3% at 0-90%, ±5% at 90-100%
v [m/s]	wind velocity	ultrasonic anemometer, WXT 520, Vaisala	±3% or ±0.3 m/s (the greater)
K_i, L_i [W/m^2]	short- and long-wave radiation flux densities	rotatable CNR-1 & CNR-4 radiometers, Kipp & Zonen	

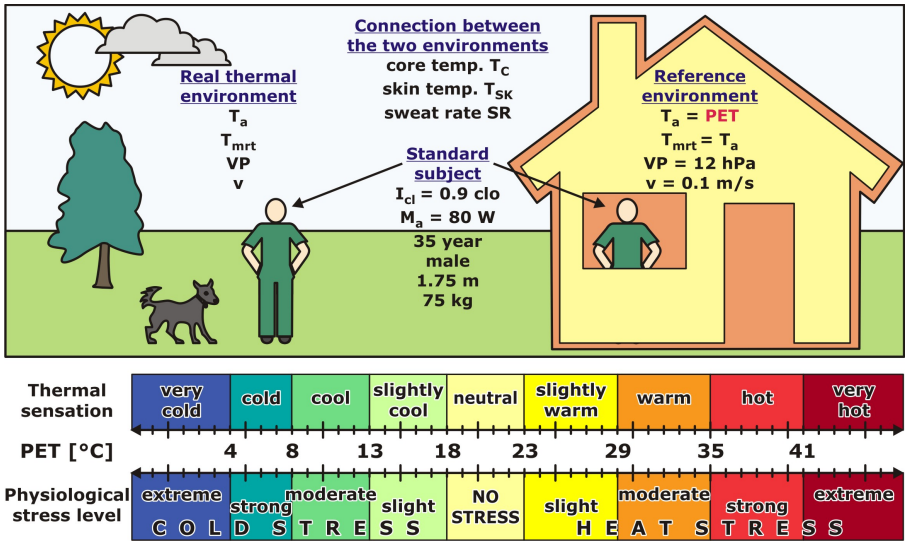

Figure 2: Explanatory figure for the *PET* and the internationally used threshold values reflecting different grades of physiological stress (constructed according to [14, 33, 34]).

Normally the arm of the net radiometer points south, and the two pyranometers and two pyrgeometers measure the corresponding short- and long-wave radiation flux densities from the upper and lower hemisphere (K_u, K_d, L_u, L_d). However, from human-biometeorological point of view not only vertical radiation flux densities, but also horizontal ones, are of interest. The rotatable arm of the net radiometers allowed us to measure horizontal radiations from the cardinal directions. After 3-minute measurement in the normal position ('U'), we rotated manually the net radiometers into the second position ('E') where they recorded K_i and L_i from east and west (K_e, K_w, L_e, L_w). Following another 3-minute measurement interval, we pointed the arms east (into the 'S' position) to measure K_i and L_i from south and north (K_s, K_n, L_s, L_n). Considering the 10 am to 6 pm measurement period, this procedure meant 160 rotations per day for each station. In order to take care for the sensors' response time and for the time delay due to the manual rotation, we deleted every first flux density data that was recorded following a rotation.

2.2 The applied human-biometeorological indices

The aim of our study is to demonstrate that air temperature is not the only cause of thermal stress outdoors. In order to achieve this goal, we calculated human-biometeorological indices that are indicative of human health and well-being. Firstly, using the six K_i and six L_i flux densities from three consecutive instrument rotations, we calculated the Mean Radiant Temperature (T_{mrt} [°C]). This measure expresses the thermal effect of the 3D radiant environment on a degree Celsius scale [31]. We utilized Höppe's equation [32] to derive T_{mrt} values:

$$T_{mrt} = \sqrt[4]{\frac{\sum_{i=1}^{6} W_i \cdot (a_k \cdot K_i + a_l \cdot L_i)}{a_l \cdot \sigma}} - 273.15,$$

where a_k and a_l are the radiation absorption coefficients of the clothed human body in the short- and long-wave domain (with 0.7 and 0.97 values, respectively), σ is the Stefan-Boltzmann constant ($5.67 \cdot 10^{-8}$ W/m^{2}K^4) and W_i is the direction-dependent weighting factor. Assuming a standing reference subject, W_i is 0.06 for the vertical and 0.22 for the horizontal directions [32].

We also calculated the Physiologically Equivalent Temperature (*PET* [°C]) to express the overall physiological effect of all thermal parameters (air temperature, air humidity, wind velocity, mean radiant temperature) on the human body [33, 34]. *PET* can be interpreted as the air temperature (T_a) of a typical indoor environment (with $T_{mrt} = T_a$, VP=12 hPa, v=0.1 m/s) in which the human body experiences the same level of thermal stress - and consequently has the same physiological reactions, resulting in the same body core temperature T_c and skin temperature T_{sk} and sweat rate SR - as in the real outdoor environment, which can be described with various T_a, T_{mrt}, VP and v values (Figure 2).

Figure 2 indicates the commonly adopted heat stress and thermal sensation threshold values of *PET* that refer to a typical Central-European subject [14]. The standard subject of the human-biometeorological investigations is

usually a 35 year old, 1.75 m height, 75 kg male (his basic metabolism is around 84 W) who performs light activity with an active work metabolism Ma of 80 W and who wears a typical suit with a thermal insulation I_{cl} of 0.9 clo [12, 33, 34].

2.3 Analysis

Each day, we installed the instruments 10-20 min prior to our dedicated measurement period to allow sensors to stabilize. In our analysis, we only used those air temperature, air humidity and wind velocity measurements that fell into the 10 am - 6 pm interval. In the case of radiation fluxes, the first values following each rotation were deleted.

We apply box-plot diagrams to illustrate the distribution of parameters and the differences between the two measurement locations. Similarly to [24], we analyze the differences between 'under tree' and 'in the sun' locations based on their median values rather than their arithmetical means. Compared to medians, mean values are very sensitive to outlier values. In order to describe the spread of the sample, we utilize the interquartile range (IQR), which is the middle 50 percent of values spreading between the lower and upper quartiles.

3 Results

3.1 Human-biometeorological differences

The five measurement days can be characterized with almost clear - partly cloudy (but not overcast) sky conditions, strong global radiation around noon and by 24-31°C maximum air temperature in the early afternoon hours. These conditions are characteristic to summer in Szeged. In order to illustrate the temporal behavior of parameters observed and calculated from measurements in the sun and under tree, we selected the measurement day of May 20th 2015 for the detailed analysis (Figure 3, Figure 4). The box plots on Figure 5 summarize the distribution of all human-biometeorological parameters measured on the five days between 10 am and 6 pm. The daily distribution of these parameters is presented in Appendix 3.

Figure 3 shows that while the air temperature difference between the two nearby measurement locations is rather small, significantly different PET values characterize the conditions in the sun and under tree on a sunny day like May 20th. Standing in the sun, the human body is subjected to a serious human-biometeorological stress. While T_a reached 30°C in the late afternoon only, PET in the sun remained above 30°C for most of the day, signaling at least a moderate heat stress. The physiological stress level was strong most of the time and for a few hours it reached the extreme level. Over the same period, a human standing under the canopy of the large tree only experienced slight to moderate heat stress (Figure 3).

In order to better understand the human-biometeorological differences between the two locations, we analyze the micrometeorological parameters separately (Figure 4). In the sun, the global radiation reached 900 W/m^2 around noon (K_u: short-wave radiation from the upper hemisphere). The fluctuation of the presented values is the result of small clouds that occasionally disturbed our measurements (Figure 4a). The most obvious effect of a tree is its shade, the reduction of global radiation, which is the function of crown transmissivity. In our case, shading results in significantly lower K_u values that fluctuate between 100-400 W/m^2 before 3 pm and remain at the constant level of 100 W/m^2 after this time.

On May 20th, 2015, the wind velocity was around 1.5-2 m/s during the observation period without considerable differences between the sunny and the shaded location (Figure 4b). Considering all v data collected over the five days (Figure 5), we have not found differences between the medians (1.3 m/s) and upper percentiles (1.7 m/s) at the two measurement points. In the case of the lower percentile, wind velocity was only slightly higher under tree than in the sun (1.1 vs. 1.0). As the locations had very similar ventilation conditions, there was no difference between their mean velocity values.

On the evaluated day, the air temperature increased by six degrees from 23 to 29°C in the 10 am - 2 pm period and remained between 29-30°C during the afternoon (Figure 4c). In line with the increase in air temperature, relative humidity decreased from 60% to 30% and reached its daily minimum at 3 pm. In contrast, vapor pressure decreased only slightly during our observation period. The differences between the two measurement points are clear but rather small: at the shaded location, air temperature run below and humidity above the corresponding values observed at the sunny location (Figure 4c).

Focusing on median differences derived from the five measurement days, we found 0.5°C lower air temperature in the shade of the tree with grassy surface compared to the sunny location with artificial pavement (Figure 5). Data also revealed slight differences in terms of air humidity: the relative humidity was 2% higher under the tree and the corresponding difference in vapor pressure was 0.4 hPa. As mentioned above, much greater and more important differences were found the human-biometeorological point

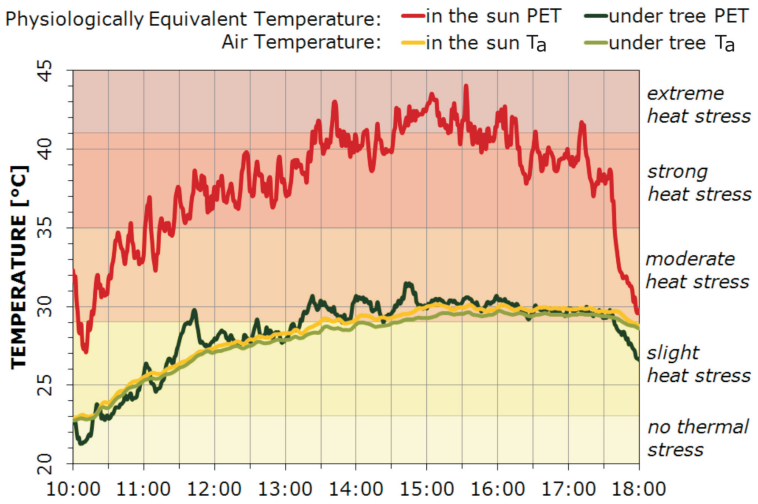

Figure 3: Temperature curves of the two measuring points on a clear day (20-May-2015) in Szeged indicate slight T_a differences, but large PET differences.

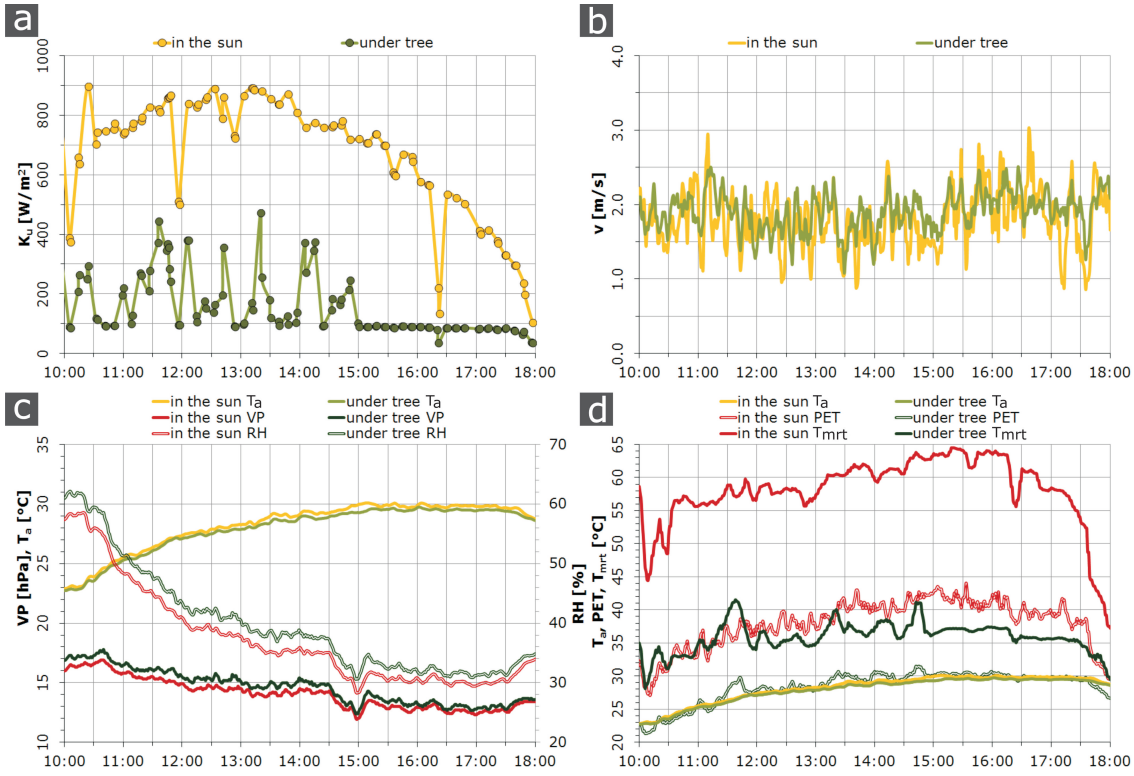

Figure 4: Temporal change of meteorological and human-biometeorological parameters measured under tree and in the sun on 20-May-2015 in Szeged.

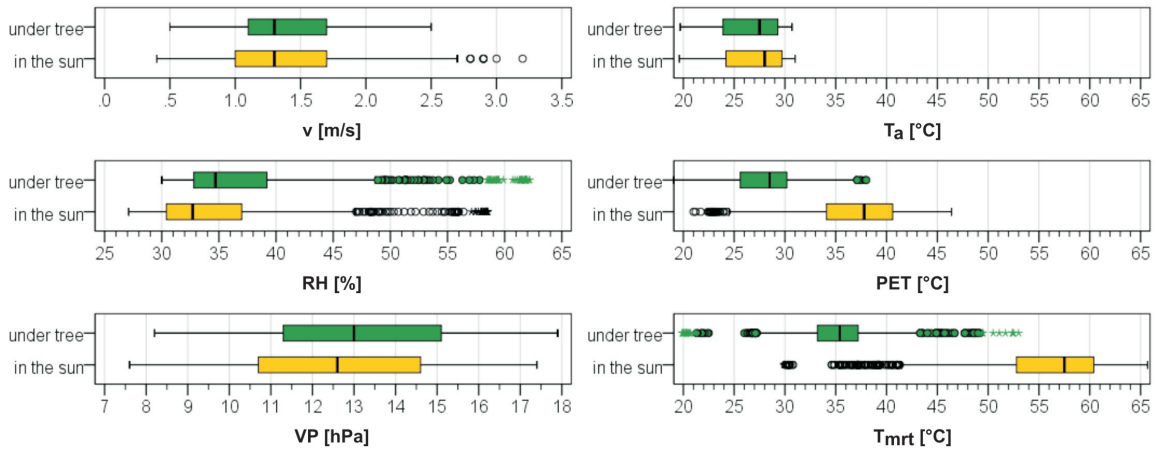

Figure 5: Meteorological and human-biometeorological parameters measured under tree and in the sun on five warm days in Szeged.

of view: the large tree reduced T_{mrt} generally by 20.1°C and PET by 9.3°C (Figure 5). This difference means a significantly lower physiological stress on the human body, which translates to the reduction of heat stress by two categories (Figure 2). Moreover, the interquartile range of PET in the sun overlaps almost perfectly with the spread of the strong heat stress category. The presence of a large tree canopy reduced these severe conditions to the level of slight heat stress (Figure 5).

There is a gradual difference among the parameters with °C units following the relationship of $T_a < PET < T_{mrt}$ (Figures 4d-5). Differences between the measurement locations increase in a similar manner: while there is almost no difference between the T_a values at the unshaded and the shaded locations, PET and T_{mrt} values are higher in the sun than under tree - offering evidence both for the cooling effect of shade trees and for the significance of radiation reduction in human thermal comfort. The reduced inter quartile ranges (IQR) of PET and T_{mrt} under tree also indicate the effect of shade trees on human-biometeorological conditions.

Figure 4d shows that on a sunny day in a sunny location PET fluctuates between the lower T_a and the higher T_{mrt} values. In the sun, T_{mrt} was above 55°C for seven hours and approached 65°C around 3-4 pm. This was the most severe heat stress period of the day (Figures 3-4d). In the shade, PET fluctuated around the measured T_a depending on wind velocity and humidity conditions (Figure 4d). In summary, PET was highly influenced by T_{mrt}. The most straightforward evidences for this are the corresponding peaks of T_{mrt} and PET values measured under the tree (see e.g. the peeks around 11.40 am, 1.20 pm and 2.45 pm on Figure 4d).

3.2 Differences in the radiation budget

Because of the overwhelming influence of T_{mrt} on PET, especially in summer days, we compared the radiant flux density components observed at the shaded and the sunny location. Figure 6 shows the temporal courses of all measured short- and long-wave radiation flux densities from all six directions separately for May 20th.

The close to clear sky conditions resulted in nearly smooth curves at the sunny point. As a result of the high sun elevation, K_u was the most important in magnitude and had a nearly bell-shaped temporal curve with a maximum of about 900 W/m^2 (Figure 6a). The curve of K_s was quite similar with lower values and with a maximum below 550 W/m^2. (Other time of the year, when the sun elevation is lower, K_s may show greater values than K_u). K_e values dominated the morning, while K_w values dominated the afternoon short-wave radiation budget. K_n was the least significant among the lateral flux densities and similar to K_d (the short-wave radiation reflected from the ground) remained around 100 W/m^2 though the whole period.

Compared to short-wave flux densities (K_i), long-wave radiation flux densities (L_i) at the sunny location did not exhibit a remarkable temporal course and their values remained closer to each other (Figure 6b). As short-wave radiation gradually warmed up the pavement, the radiation from this surface became the dominant long-wave radiation component in the case of the sunny location. L_d increased slowly from 500 to 575 W/m^2 in the first half of the measurement, than it plateaued between 1.30 pm and 4 pm, only to fell back to 525 W/m^2 for the remaining period. Since the sunny measurement point had no vertical obsta-

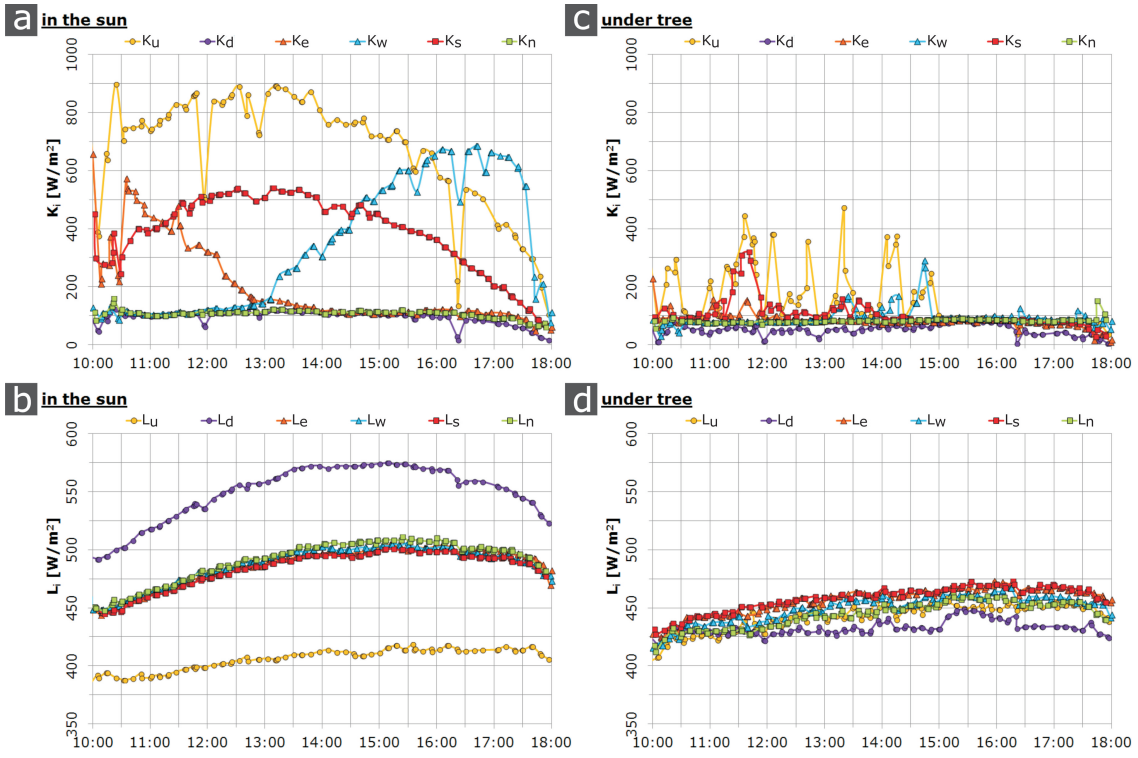

Figure 6: Short- and long-wave radiation flux densities measured from different directions in the sun and under tree on 20-May-2015 in Szeged, Hungary.

cle in its vicinity that could serve as heat radiating surface, the lateral long-wave components had similar values and remained well below the magnitude of L_d. L_u, the atmospheric counter radiation from the upper hemisphere, remained the lowest with around 400 W/m^2 (Figure 6b).

The charts on the right side of Figure 6 illustrate the effect of shade tree on different K_i and L_i flux densities. The large canopy reduced K_i values by a great extent (Figure 6c), especially after 3 pm when shading was most effective. L_i were also modified (Figure 6d): the flux density values from different directions remained rather similar and generally lower than those at the sunny location. This is due to the shaded grassy surface, which remained relatively cool and did not become an effective source of L_d. Compared to the sunny location, only L_u values have increased since the tree canopy emitted more radiation and was closer to the sensor than the 'cold' sky in the other case (Figure 6d).

Figure 7 summarizes the distribution of the measured radiation flux densities over the five measurement days. In the case of short-wave radiation in the sun, the upper flux density K_u had the highest median (679 W/m^2). Second to it were K_s and K_w with 352 W/m^2 and 257 W/m^2 median values respectively. K_e, K_n and K_d remained much lower during the studied period (131 W/m^2, 110 W/m^2 and 97 W/m^2). Due to the shading of the tree canopy, K_u decreased the most - its median dropped from 679 W/m^2 to 115 W/m^2 (-83%). In the case of K_d the decline was only 48 W/m^2 (-49%). In the lateral directions, the reduction is also considerable, especially in K_s and K_w that can be attributed to the extensive tree canopy. (Note that if we had performed our measurements through the entire daytime, the distribution of K_e and K_w flux densities would have been similar to each other and to K_s. However, due to our measurement design, the afternoon hours and thus the western flux densities are more pronounced.) Compared to other directions, the north-facing sensor did not receive much radiation and thus the reduction in K_n owing to the presence of shade tree is rather modest (-26%). It should be noted that both the spread of short-wave flux densities in the sun and their reduction due to tree shading depend on the cloud coverage: not only higher flux densities, but also pronounced reductions can be observed during sunny conditions, while the effect of shading is greatly reduced in cloudy or overcast conditions.

The distributions of the long-wave radiation flux densities measured from different directions are more similar to each other (note, the scale is narrower on the right side charts of Figure 7). Due to the warm pavement in the sunny location, L_d has the highest median (553 W/m^2),

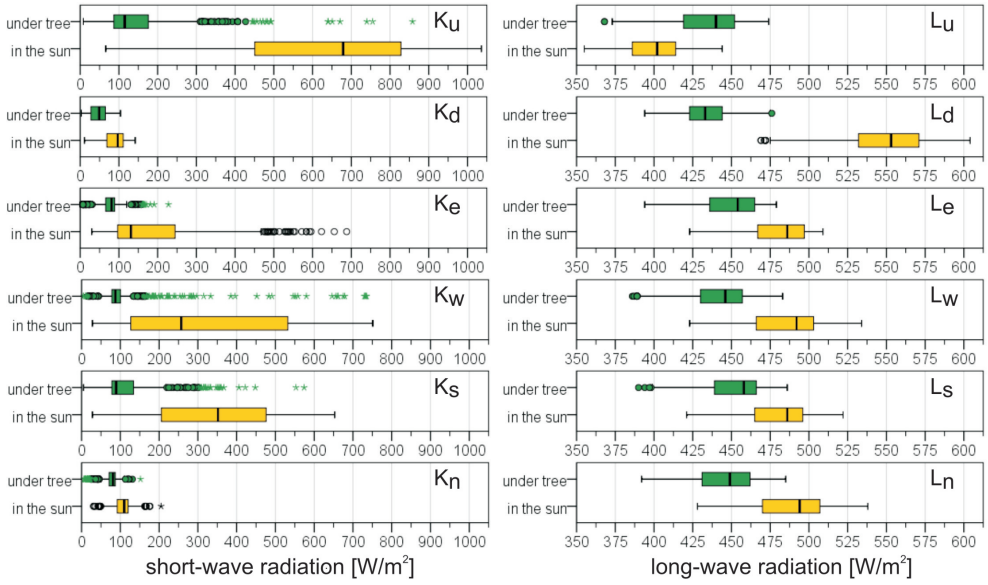

Figure 7: Radiation flux densities measured under tree and in the sun on five warm days in Szeged.

while L_u has the lowest (402 W/m^2). At the sunny location, lateral long-wave radiation components have a median of around 480-490 W/m^2. The shade from the tree canopy reduced almost every L_i, which resulted in similar median values. The only exception is L_u that increased slightly due to the presence of the tree. As already mentioned, this phenomenon is because the tree canopy is closer and it is a more effective heat-emitting surface than the clear sky. Nevertheless, the L_u-enhancing effect of the tree is greatly compensated by the reduction in L_d (-120 W/m^2; -22%) and the decline of the lateral L_i (-6 to 9%). Owing to the presence of the tree, the reduction of the IQR of long-wave flux densities is smaller than in the case of the short-wave flux densities (Figure 7). The modifying effect of a large shade tree on the six K_i and six L_i radiation flux densities are graphically summed up on Figure 8.

Figure 9 illustrates the distribution of the radiation flux densities absorbed by a standing human body. These absorbed flux densities affect directly the magnitude of T_{mrt}. Compared to the original flux densities in Figure 7 these are already weighted with the wavelength-dependent absorption coefficients and with the direction-dependent projection factors. (They can be calculated as follows: $K_i^* = K_i \cdot W_i \cdot a_k$, $L_i^* = L_i \cdot W_i \cdot a_l$.) Due to these transformations, the hierarchy of flux density magnitudes (K_i^* and L_i^* on Figure 9) changed drastically compared to the originally measured ones (K_i and L_i on Figure 7):

- Firstly, the contribution of the long-wave components (L_i^*) increased because of the higher absorption coefficient in this wavelength, compared to that in the short-wave domain (a_l: 0.97, a_k: 0.7).
- Secondly, the horizontal flux densities became more important, while the significance of the vertical flux densities decreased owing to the positional weighting factors (lateral: 0.22, vertical: 0.06).

4 Discussion

Summertime thermal stress mitigation via landscape design should be one of the most intensively studied issues of urban human-biometeorology [9, 28]. Planting trees for shading and evaporative cooling may seem axiomatic and a simple 'tool' in the hand of urban planners for mitigating thermal stress in regions with long and warm summers [10, 26]. However, there is a need for studies that offer empirical data on the shading capacity as well as on the heat stress reduction potential of these natural landscape elements [24, 29]. In order to aid the work of landscape designers and to fill this research gap, we offer evidences on the beneficial human-biometeorological effect of large urban trees in summertime within the context of Hungary.

Although we found differences in basic micrometeorological parameters between the two measurement locations (lower air temperature and higher humidity under the tree), the general level of T_a-reduction remained below 1°C. In contrast, *PET* - the human-biometeorological index - was almost 10°C lower under the tree. During early summertime conditions, this means that the body is ex-

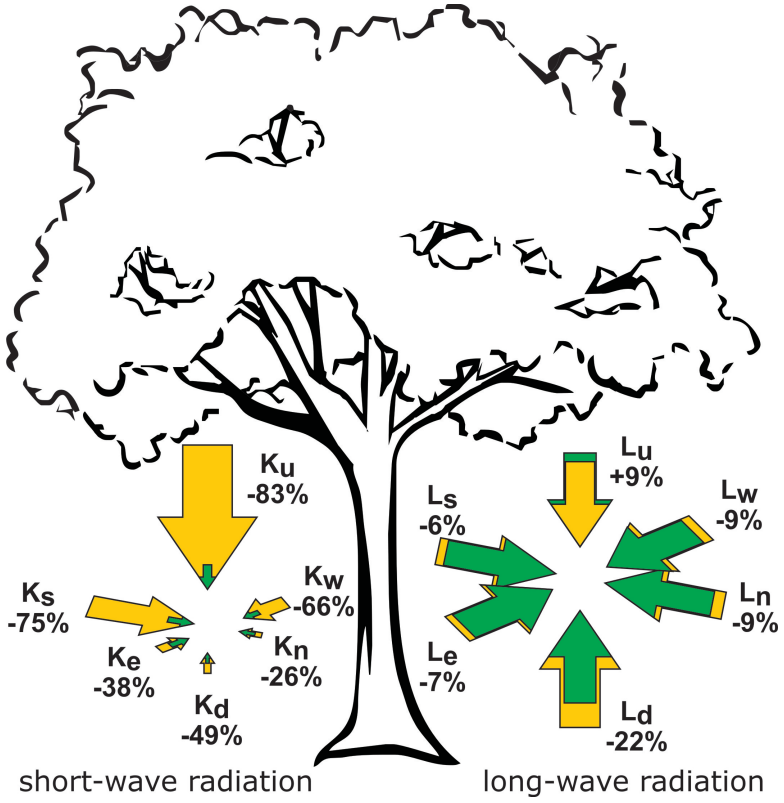

Figure 8: Radiation modification effect of the investigated *Sophora japonica* in the short- and long-wave domain: yellow arrows represent radiation flux densities in the sun, while green arrows are for them under the tree.

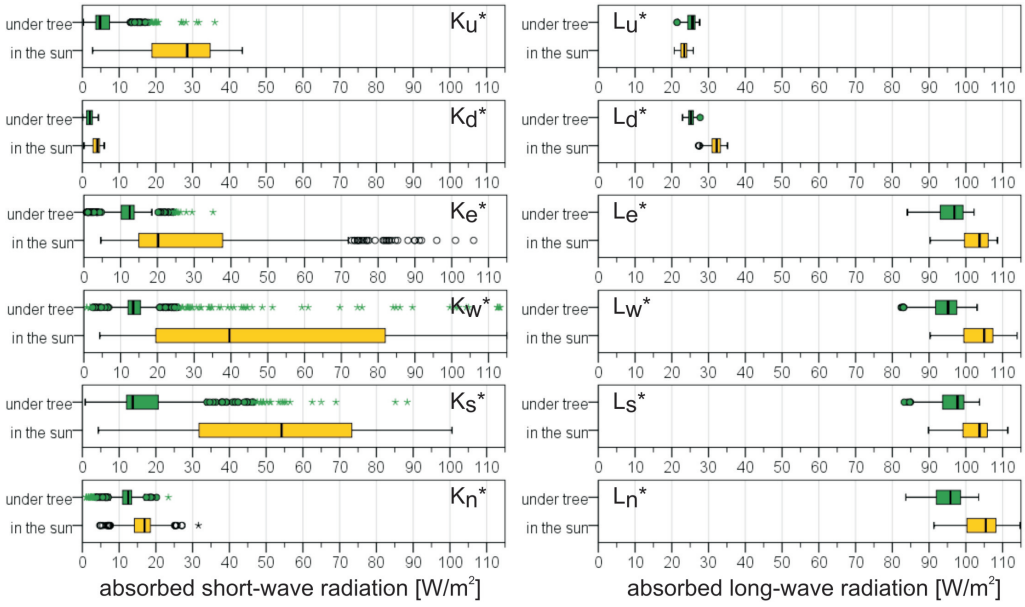

Figure 9: Radiation flux densities absorbed by a man in standing position under tree and in the sun on five warm days in Szeged.

posed to slight heat stress levels as opposed to strong heat stress levels in a sunny location. We must emphasize that our measurement days did not include really hot summer days and most of our days are characterized with partly cloudy sky. On really hot summer days, these differences would be more significant reducing extreme level of heat stress to moderate one; see for example the work of [28].

As neither air temperature, nor air humidity differences were great enough to account for the human-biometeorological differences observed between the two measurement sites, our results indicate that 3D radiant environment plays a key role in forming outdoor heat stress on warm, sunny days. This is in accordance with the outcome of earlier studies in Central-Europe [18, 28]. Influenced by changing sky conditions, T_{mrt} also showed remarkable fluctuations at the open location. Nevertheless, we found considerable differences between the two measurement sites. Likewise as [18] we analyzed every component of the radiation budget separately, to demonstrate the background mechanisms of these human-biometeorological differences.

While long-wave radiation components have greater impact on the magnitude of the evolved radiation load (T_{mrt}), the tree's modification effect was greater in the short-wave domain. However, as a consequence of the reduced short-wave flux densities, long-wave flux densities decreased as well. Basically, the tree crown reduced the amount of short-wave radiation reaching both the body and the ground from the upper hemisphere. Consequently, the tree shade also lowered the reflected radiation from the ground. Furthermore, the large canopy also reduced the lateral short-wave flux densities from southern, western, and eastern directions.

Under the tree, the ground surface was not able to heat up so much because of the reduced short-wave radiation. Consequently, it emitted less radiation in the long-wave domain. (In the case of our study, the grassy surface also contributed to lower surface temperature values under the tree.) Overall, the effect of lowered short- and long-wave flux densities under the tree more than compensated for the slight increase in the long-wave radiation from the upper hemisphere.

It is important to briefly discuss the effect of body posture on the observed differences. The human-biometeorological evaluation of the thermal environment relies on a standardized subject, which is most frequently assumed to be in standing position [9, 18, 28, 29]. As a result, we used 0.06 weighting factors for the vertical and 0.22 for all lateral radiant flux densities. It should be emphasized that because of this assumption, our analysis of the radiant flux density components contributing to the T_{mrt} and PET are only valid for standing persons. However, based on our human monitoring data that was collected simultaneously with the measurements, most people either sat on benches or lay on the grass. In the case of these subjects, the importance of the vertical flux densities increases at the expense of the horizontal ones. Moreover, the surface temperature of benches and the ground becomes more important, because of the direct contact people have with these surfaces. Standing posture and the corresponding weighting factors are appropriate in street canyons, while in squares and parks - where people tend to spend more time - every posture can be important. The dominant type of body posture depends on the design and function of the area (street, square, park). Standing postures characterize active pursuits (e.g. walking, sports), while sitting or lying posture imply passive (e.g. reading, chatting, eating) activities.

The microclimate regulation potential of trees depends on the spatial distribution of vegetation: isolated trees have smaller effect than groups of trees [24]. Additionally, age and specie-related characteristics - such as leaf area, crown shape and the structure of canopy - are also important factors that influence shading and the consequent small-scale human-biometeorological impact. These factors also change with time and with the deterioration of the trees' health [35]. Decline in health is more pronounced when the tree specimen does not tolerate the harsh urban environment or does not demonstrate resilience to other local conditions [36]. Climate conscious planning, preliminary site assessment and prudent selection of species (or cultivars) support the health of the planted trees and ensure that they can offer the full spectrum of their ecosystem services.

The presented study offers data and analysis on the small-scale human-biometeorological regulation services of a mature urban tree. We hope that our contribution to the knowledge on the thermal stress mitigation effect of urban trees will help landscape planners to design 'successful' outdoor spaces that will be more comfortable and used more frequently by citizens.

Acknowledgement: The authors would like to thank for Ágnes Gulyás and Márton Kiss that they introduced us in the literature of ecosystem services of urban trees. We are grateful for Csilla Gál for the English language revision, and for the two Reviewers for their constructive suggestions that contributed significantly to the value of this paper.

References

[1] Meehl G.A., Tebaldi C., More intense, more frequent, and longer lasting heat waves in the 21st century. Science, 2004, 305, 994-997.

[2] Koffi B., Koffi E., Heat waves across Europe by the end of the 21st century: multiregional climate simulations. Climate Res., 2008, 36, 153-168.

[3] Gosling S.N., Lowe J.A., McGregor G.R., Pelling M., Malamud B.D., Associations between elevated atmospheric temperature and human mortality: a critical review of the literature. Climatic Change, 2009, 92, 299-341.

[4] Yu W., Mengersen K., Wang X., Ye X., Guo Y., Pan X. et al., Daily average temperature and mortality among the elderly: a meta-analysis and systematic review of epidemiological evidence. Int. J. Biometeorol., 2012, 56, 569-581.

[5] Potchter O., Ben-Shalom H.I., Urban warming and global warming: Combined effect on thermal discomfort in the desert city of Beer Sheva, Israel. J. Arid Environ., 2013, 98, 113-122.

[6] Zuvela-Aloise M., Bokwa A., Dobrovolny P., Gál T., Geletic J., Gulyás Á. et al., Modelling urban climate under global climate change in Central European cities. Geophysical Research Abstracts, Vienna, Austria, 2015, Paper EGU 2015-1594.

[7] Eliasson I., The use of climate knowledge in urban planning. Landscape Urban Plan., 2000, 48, 31-44.

[8] Mills G., Progress toward sustainable settlements: a role for urban climatology. Theor. Appl. Climatol., 2006, 84, 69-76.

[9] Mayer H., KLIMES - a joint research project on human thermal comfort in cities. Ber. Meteor. Inst. Albert-Ludwigs Univ. Freiburg, 2008, 17, 101-117.

[10] Erell E., Pearlmutter D., Williamson T.J., Urban microclimate: Designing the spaces between buildings. Earthscan, London, 2011.

[11] Gill S.E., Handley J.F., Ennos A.R., Pauleit S., Adapting cities for climate change: the role of the green infrastructure. Build. Environ., 2007, 33, 115-133.

[12] Madureira H., Andersen T., Planning for multifunctional urban green infrastructures: Promises and challenges. Urban Des. Int., 2014, 19, 38-49.

[13] Bowler D.E., Buyung-Ali L., Knight T.M., Pullin A.S., Urban greening to cool towns and cities: A systematic review of the empirical evidence. Landscape Urban Plan., 2010, 97, 147-155.

[14] Matzarakis A., Mayer H., Iziomon M.G., Application of a universal thermal index: physiological equivalent temperature. Int. J. Biometeorol., 1999, 43, 76-84.

[15] Gulyás Á., Unger J., Matzarakis A., Assessment of the microclimatic and human comfort conditions in a complex urban environment: modelling and measurements. Build. Environ., 2006, 41, 1713-1722.

[16] Ali-Toudert F., Mayer H., Effects of asymmetry, galleries, overhanging façades and vegetation on thermal comfort in urban street canyons. Sol. Energy, 2007, 81, 742-754.

[17] Toy S., Yilmaz S., Yilmaz H., Determination of bioclimatic comfort in three different land uses in the city of Erzurum, Turkey. Build. Environ., 2007, 42, 1315-1318.

[18] Mayer H., Holst J., Dostal P., Imbery F., Schindler D., Human thermal comfort in summer within an urban street canyon in Central Europe. Meteorol. Z., 2008, 17, 241-250.

[19] Lin T.P., Matzarakis A., Hwang R.L., Shading effect on long-term outdoor thermal comfort. Build. Environ., 2010, 45, 213-221.

[20] Toy S., Yilmaz S., Thermal sensation of people performing recreational activities in shadowy environment: a case study from Turkey. Theor. Appl. Climatol., 2010, 101, 329-343.

[21] Hwang R.L., Lin T.P., Matzarakis A., Seasonal effects of urban street shading on long-term outdoor thermal comfort. Build. Environ., 2011, 46, 863-870.

[22] Andreou E., Thermal comfort in outdoor spaces and urban canyon microclimate. Renew. Energ., 2013, 55, 182-188.

[23] Gómez F., Pérez Cueva A., Valcuende M., Matzarakis A., Research on ecological design to enhance comfort in open spaces of a city (Valencia, Spain). Utility of the physiological equivalent temperature (PET). Ecol. Eng., 2013, 57, 27-39.

[24] Andrade H., Vieira R., A climatic study of an urban green space: The Gulbenkian park in Lisbon (Portugal). Finisterra, 2007, 42, 27-46.

[25] Shashua-Bar L., Potchter O., Bitan A., Boltansky D., Yaakov Y., Microclimate modelling of street tree species effects within the varied urban morphology in the Mediterranean city of Tel Aviv, Israel. Int. J. Climatol., 2010, 30, 44-57.

[26] Shashua-Bar L., Pearlmutter D., Erell E., The influence of trees and grass on outdoor thermal comfort in a hot-arid environment. Int. J. Climatol., 2011, 31, 1498-1506.

[27] Oliveira S., Andrade H., Vaz T., The cooling effect of green spaces as a contribution to the mitigation of urban heat: A case study in Lisbon. Build. Environ., 2011, 46, 2186-2194.

[28] Lee H., Holst J., Mayer H., Modification of human-biometeorologically significant radiant flux densities by shading as local method to mitigate heat stress in summer within urban street canyons. Adv. Meteorol., 2013, Article ID 312572.

[29] Lee H., Mayer H., Schindler D., Importance of 3-D radiant flux densities for outdoor human thermal comfort on clear-sky summer days in Freiburg, Southwest Germany. Meteorol. Z., 2014, 23, 315-330.

[30] WMO, Climatological Normals (CLINO) for the period 1961-1990. WMO/OMM-No 847, Secretariat of the World Meteorological Organization, Geneva, 1996.

[31] Kántor N., Unger J., The most problematic variable in the course of human-biometeorological comfort assessment - the mean radiant temperature. Cent. Eur. J. Geosci., 2011, 3, 90-100.

[32] Höppe P., Ein neues Verfahren zur Bestimmung der mittleren Strahlungstemperatur im Freien [A new method to determine the mean radiant temperature outdoors], Wetter und Leben, 1992, 44, 147-151 (in German with English summary).

[33] Mayer H., Höppe P., Thermal comfort of man in different urban environments. Theor. Appl. Climatol., 1987, 38, 43-49.

[34] Höppe P., The physiological equivalent temperature - a universal index for the biometeorological assessment of the thermal environment. Int. J. Biometeorol., 1999, 43, 71-75.

[35] Nowak D.J., Crane D.E., Stevens J.C., Hoehn R.E., Walton J.T., Bond J., A ground-based method of assessing urban forest structure and ecosystem services. Arboriculture & Urban Forestry, 2008, 34, 347-358.

[36] Jim Y.C., Roadside trees in urban Hong Kong: Part IV tree growth and environmental condition. Arboricultural Journal, 1997, 21, 89-106.

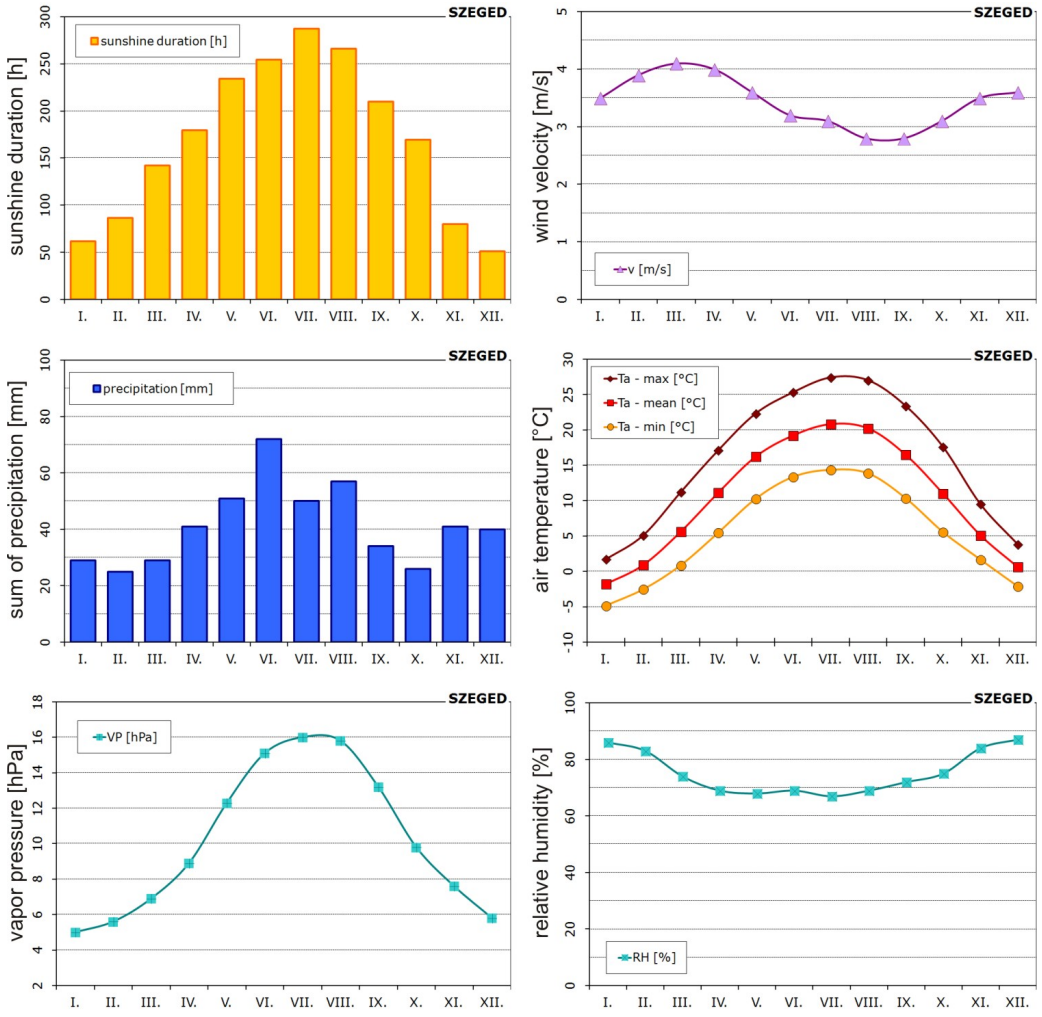

Appendix 1: Climate diagrams of Szeged based on the 1961-1990 period [30].

Appendix 2: Photos about the Dugonics Square in the city of Szeged.

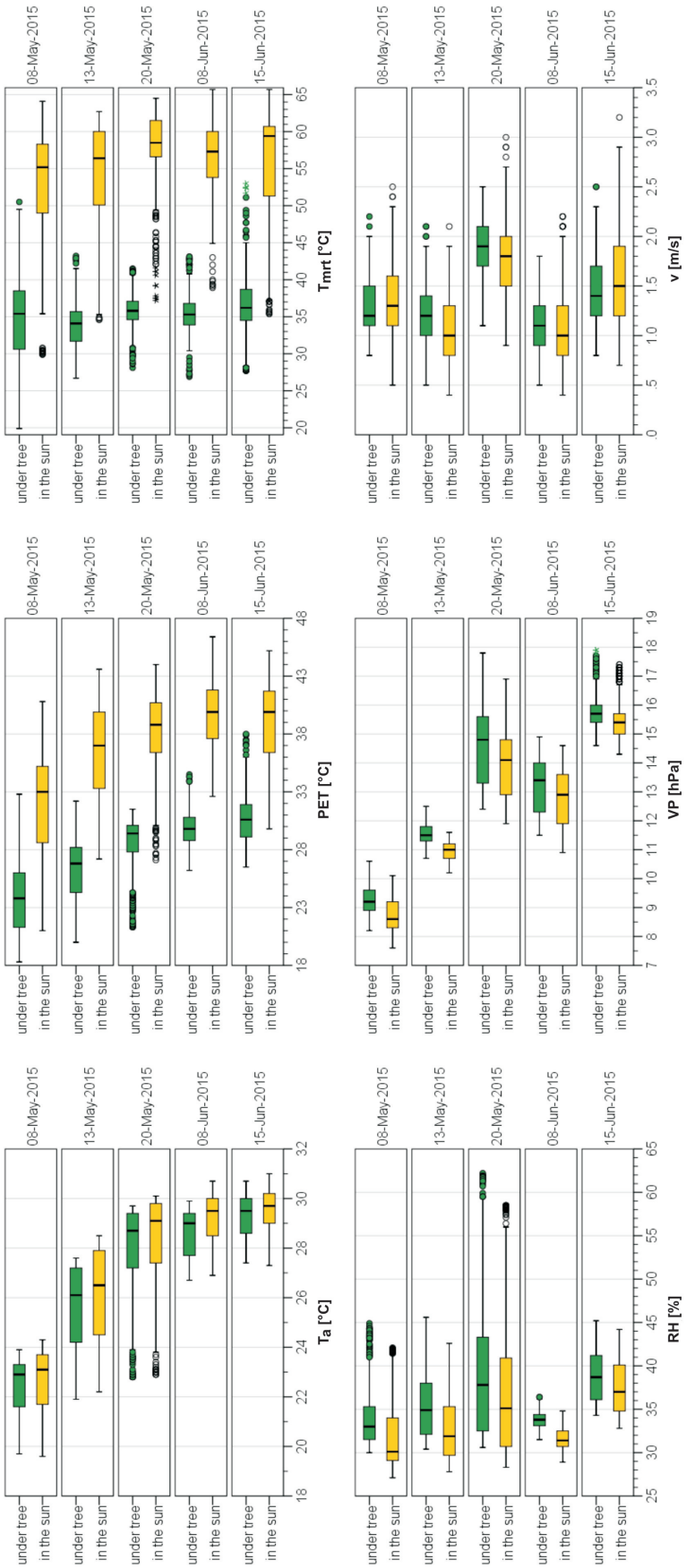

Appendix 3: Meteorological and human-biometeorological parameters measured under tree and in the sun in Szeged, separated according to the five measurement days.